Determination of the elastic properties of Graphene by indentation and the validity of classical models of indentation

K. M. Fair, M. D. Arnold, M J Ford
School of Physics & Advanced Materials, University of Technology, Sydney, NSW 2007, Australia

E-mail: Mike.Ford@uts.edu.au

Abstract. *Ab initio* and empirical force field methods are used to simulate the loading of a large graphene membrane under an indenter analogous to an atomic force microscope tip. From these calculations we attempt to resolve ambiguities around determination of the elastic constants of graphene from such indentation experiments. We investigate the effect of formation of wrinkles and more importantly the applicability of modelling the membrane as a continuous elastic sheet. By comparing both empirical potential and large scale Density Functional Theory calculations we have also assessed the performance of classical potentials in describing bending in this system. We find that the in-plane Young's modulus deduced from the indentation simulations using the classical expression for a clamped elastic membrane under a central point load is not consistent with that calculated directly by from the in-plane stress-strain curve.

PACS: 31.15.A-, 62.20.de, 62.20.F-, 68.65.Pq

1. Introduction

The discovery of graphene as a stable isolated 2D sheet in 2004[1] can be considered a major land mark of modern material science. Its unique electrical[2], optical[3] and mechanical properties[4] promise many diverse applications[5–8]. The characterization of graphene is essential to exploiting its full potential and has been of considerable interest in recent literature[9–11]. One interesting aspect of graphene is its considerable mechanical strength as it is thought to have one of the highest values of effective Young's modulus. This can be understood by the work of Griffith in 1921[12] who concluded that the breaking strength of a brittle material is not determined only by the intrinsic strength of its atomic bonds but the size of is defects and flaws. The first experimental determination of graphene's intrinsic strength did so in terms of the two-dimensional Young's modulus, E^{2D} [4], this quantity, in units of force per unit length, can be converted to the conventional Young's modulus, in units of pressure, by assuming an effective thickness equal to the interlayer spacing in graphite[13]. The Young's Modulus was obtained by indentation of a suspended graphene sheet with an atomic force microscope (AFM) in non-contact mode, with the results analysed by approximating the system as an isotropic clamped circular membrane under central point loading using the model[4,14,15]:

$$F = \sigma_0^{2D} \pi a \left(\frac{\delta}{a}\right) + E^{2D} (q^3 a) \left(\frac{\delta}{a}\right)^3 \qquad (1)$$

where F is the applied force, δ is the indentation depth, σ_0^{2D} is the pretension in the film, a is the membrane diameter and q is a dimensionless constant, $q = 1/(1.05 - 0.15v - 0.16v^2)$ with v Poisson's ratio.

At small indentation, where the induced stress is comparable to the pretension in the membrane, the first term in this model dominates. At large indentation, the second term dominates, pretension supposedly has little influence and the membrane deforms. There are a number of assumptions

underlying this model: the bending rigidity can be ignored; the membrane is isotropic both in-plane and across its thickness the induced stress is isotropic that is radial and tangential components are equal and are independent of radial distance from the film centre. The assumption that out of plane effects can be neglected for graphene membranes is based on previous *ab initio* work [16,17] that suggested the energy change from out of plane stretching is three orders of magnitude smaller than that of the in-plane stretching. Using this model, simulations yield a scatter of values for the Young's modulus from 247, 268, 552 Nm^{-1} [18–20]. This disparity warrants testing of the continuum models applicability in a more direct way.

It has been reported from classical force-field molecular dynamics simulation that graphene's bending rigidity is dependent on sheet deflection [21,22]. Additionally it has been suggested for the centre point load indentation of a circle with a fixed edge there should be a natural formation of wrinkles in the graphene beyond some critical indentation[23]. Wrinkling in flat graphene has recently been attributed to the presence of in-plane strain [24,25], however, there appears to be some discussion in the literature about the existence of wrinkles during indentation[20,26], with limited information concerning the influence on the calculated Young's modulus. To our knowledge, there are no first principles simulations of the load vs indentation relationship for out-of plane deformation as in the experiment of Lee et al [4]. Existing studies have focused either on continuum[23,27–29], empirical models[18–20,26], or *ab initio* models that consider only in-plane strains[30–32] in a small unit cell. This is likely due to the computational expense associated with simulations on the scale of the indentation experiments.

This paper presents first principles calculations of graphene's elastic properties and mechanical response to indentation with the membrane under either compressive or tensile strain prior to indentation (pretension). These large, membrane calculations have been carried out at both the Density functional Theory level and using empirical potentials. The in-plane linear and non-linear elastic constants are first calculated directly within the framework of Density Functional theory for a small, 4 atom unit cell under in-plane strain. The elastic properties under indentation are then calculated over a range of membrane pretensions using a large sheet containing 2160 atoms. The purpose of this is to replicate the experiments of *Lee et al* [4] to assess the validity of the classical model in the presence of pretension (both compressive and tensile) and the resulting interesting morphological effects, such as wrinkles and strain induced indentation. The model is assessed by means of the derived value of Young's Modulus and corresponding pretension.

2. Method

The relaxed unit cell used for the determination of in-plane elastic constants contains 4 atoms. The dimensions of the cell are 2.5 × 4.2 × 20 Å. The large membrane with 2160 atoms has dimensions 73.8 × 76.7 × 60 Å . The DFT calculations are performed using the SIESTA code[33,34] with the Perdew-Burke-Ernzerhof (PBE) generalized gradient approximation (GGA)[35] to the exchange-correlation functional, using a double zeta plus polarisation basis set. For the 4 (2160) atom unit cell a reciprocal-space k-point mesh and orbital confinement of 15 × 15 × 1 and 5mRy (1 × 1 × 1 and 10mRy) is used respectively. The density matrix convergence of 0.0001 and a stress tolerance of 0.05 GPa for cell relaxation is used for both unit cells. Orbital confinement is a particularly important parameter as it determines the cut-off for the orbital radii, a smaller value corresponding to more extended orbitals, but requiring greater computational effort. The values used here of 5 mRy for the small cell and 10 mRy for the large are a reasonable compromise between convergence and computing time; 10 mRy confinement represents about the limit for obtaining reasonable results. For the large membrane only the gamma-point is calculated in reciprocal space because we are effectively modelling the system as an isolated membrane. The empirical force field calculations are performed using the GULP software package[36–38] with Brenner potentials[39,40] for the intra atomic forces of the graphene. For the interaction of the indenter to the graphene a Lennard-Jones potential, $U(r) = 4\epsilon[(\sigma/r)^{12} - (\sigma/r)^{6}]$, is applied with arbitrary small potential well, ϵ, positioned at, σ, ~6Å and a real space cut off of 8.89Å.

To calculate the Young's modulus from the small cell directly, the variation in energy density under applied in-plane strain is calculated in order to determine the second and third order elastic constants (C_{ij}, C_{ijk}) of graphene. Because of its symmetry graphene has just two unique second order (C_{11}, C_{12}), and three unique third order ($C_{111}, C_{112}, C_{222}$) elastic constants. These values are calculated from the energy density of the 4 atom cell as a function of uniaxial strain along the zigzag edge (zz), armchair edge (ar) and a combination of both, namely hydrostatic planar (hp) strain. In each strained system the atoms are allowed to relax with a force tolerance of 0.04eV/Ang, within the fixed cell.

To simulate a graphene sheet indented by an AFM analogous to the experiment of *Lee et al*[4] a circle within an approximately square sheet is conically deformed in the z-axis, a diamond 'indenter' is then placed in the well of the indentation several angstroms above the cones centre. An empirical force field geometry optimisation is then performed using the bond order Brenner potential for the intra-atomic forces of the graphene with a long range Lennard-Jones potential between the indenter and the graphene. During this indentation the graphene outside the indented circle and the diamond indenter remain geometrically constrained. The depth of indentation is taken to be the distance along the z-axis from the plane of the graphene outside the well to the lowest point of the indented graphene. This replicates the conditions of a graphene sheet sitting atop a substrate well experiencing an indentation from an AFM tip. This methodology was modified slightly for the DFT calculations of the large membrane as it is prohibitively expensive to perform the full geometry optimisation at this level. Instead optimised geometries from the empirical calculation above are used with the lattice constant stretched by 1 % and a single-point DFT calculation performed. From small cell calculations we find that geometry optimisations with DFT and the Brenner potential differ by 1 %.

3. Results and discussion

The results of strain calculations for the small unit cell are shown in figure 1, where the energy density relative to the unstrained cell is plotted as a function of in-plane strain. Notice how these curves are quite asymmetric indicating that graphene is non-linear in its elastic response even at quite small strain values. This is consistent with previous tight binding atomistic calculations[30,31]. These calculations have also been performed at the empirical level using the Brenner potential, the results are qualitatively similar and are not shown here. From a polynomial fit of the strain vs energy density curves in figure 1 it is possible to obtain the second and third order elastic constants via the relationships [30,31]

$$\frac{\Delta E(\eta_{zz})}{S} = E_0 + \frac{1}{2}C_{11}\eta^2 + \frac{1}{6}C_{111}\eta^3 \qquad (2.1)$$

$$\frac{\Delta E(\eta_{ar})}{S} = E_0 + \frac{1}{2}C_{11}\eta^2 + \frac{1}{6}C_{222}\eta^3 \qquad (2.2)$$

$$\frac{\Delta E(\eta_{hp})}{S} = E_0 + (C_{11} + C_{12})\eta^2 + \frac{1}{6}(4C_{111} - 2C_{222} + 6C_{112})\eta^3 \qquad (2.3)$$

Where $\frac{\Delta E(\eta)}{S}$ is the energy density of the system, E_0 is the energy of the system without strain and η is the strain, chosen in this instance to be of the Lagrangian regime[31,41]. The results of these fits are given in Table 1.

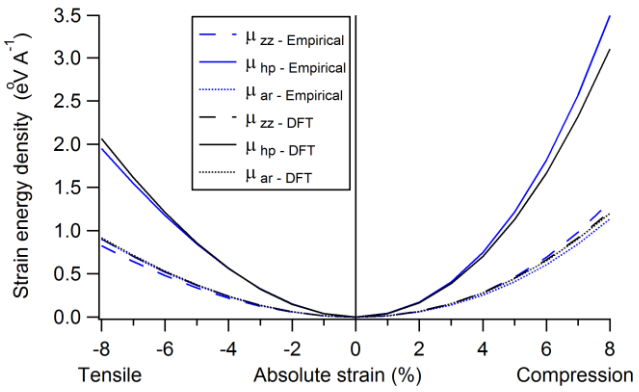

Figure 1. The DFT and empirically calculated variation in energy density for hydrostatic planar, η_{HP}, and uniaxial strain applied along the zigzag, η_{ZZ}, and η_{AR} edges.

Overall there is good agreement between our calculations and those previously published[30,31]. The Young's modulus can be derived from these elastic constants by the relationship $E = C_{11}(1 - v^2)$, we will discuss these later where we compare with our indentation simulations. Agreement between the DFT calculations and the Brenner potential is good for the second order terms but not so for the third order values. C112 is difficult to determine as it sensitive to the values of C111 and C222. We have also determined the elastic properties by indentation of a graphene membrane, analogous to the experimental measurements of Lee et al [4]. By fitting equation 1 to this data *Lee et al* determined both the Young's Modulus and pretension in the membrane and deduced that their suspended membranes are initially under tensile strain. In our calculations we consider both initial compressive and tensile strain in the membrane.

Table 1. The values for the second and third order elastic constants, as well as Poisson's ratio v, calculated from the small strain method using both *DFT* and empirical Brenner potential in comparison to other literature.

	DFT	**Empirical**	**Literature**
C11	340	348	342[a]
C12	63	93 ± 1	65[a]
C111	-2810 ± 6	-3944 ± 26	-2832[a], -2725[b]
C112	-419 ± 2	-118 ± 6	-390[a], -591[b]
C222	-2620 ± 7	-2459 ± 19	-2684[a], -2523[b]
V	0.18	0.27	0.19[a], 0.31[b]

[a] *Ab intio*[30]

[b] Semi-empirical, tight-binding atomistic simulations [31]

As might be expected the initially compressed graphene sheets are observed to spontaneously indent when we perform a geometry optimisation without the presence of the indenter tip, figure 2 (a). The depth of this indent dependent upon the pre-compression. This mechanical 'popping' effect takes place in order for the compressed sheet to minimize its strain energy and has been previously observed in simulations of low strained graphene circles [42]. Figure 2 shows the relaxed indentation profile of two graphene sheets with compression applied by reducing the lattice vectors by 3 % and 7 %. Buckling of the sheet in this way only occurs if the sheet is given a small nudge in order to break its symmetry. This process could contribute to the initial indentation observed experimentally and which is presumed to be purely due to Van de Waals forces with the sides of the well. If compressive strain were present in the sheet it would naturally be inclined to depress into the well as adhesion forces present would certainly disrupt the symmetry of the system. Interestingly it is observed that for strain greater than 3% wrinkles in the indented morphology occur which function as an additional mechanism to minimize strain energy, figure 2 (b). While these wrinkles in indented graphene have

been simulated before [26] we believe these to be the first atomistic simulations identify strain as the driving mechanism.

By moving the constrained diamond indenter down towards the centre of the unconstrained graphene circle and optimising the geometry of the graphene around the indenter, the indented structure for a particular depth is found. The associated load is then calculated from the stress tensor. We repeat this process for a range of pretensions both tensile and compressive; example load-indentation curves are given in figure 3 (a). As expected, tensile (compressive) prestrain of the membrane causes the load versus indentation curves in Figure 3(a) to shift above (below) the indentation curve without strain. We then fit the classical expression for a centre-loaded, clamped isotropic elastic sheet given in equation 1 to these load versus indentation curves to extract values of Young's modulus and pre-tension. This is a direct simulation of the experiment performed by Lee et al[4]. For compressed indentations with the popping effect there is a transfer of stress from the xx and yy components to the zz, this is treated as an offset as it is not load applied by the indenter. The indentation, however, would be observed by an AFM and so our definition of indentation depth holds.. The results of this fitting procedure are given in Table 2. It is interesting to note that with these assumptions about the popping effect the variation in young's modulus with strain appears unperturbed, i.e. symmetric compared to the variation due to tensile strain. This is the case even with the presence of wrinkles at high compressive strain. The value of Young's Modulus determined earlier from our 4 atom unit cell under in-plane strain is also given in table 2 for comparison.

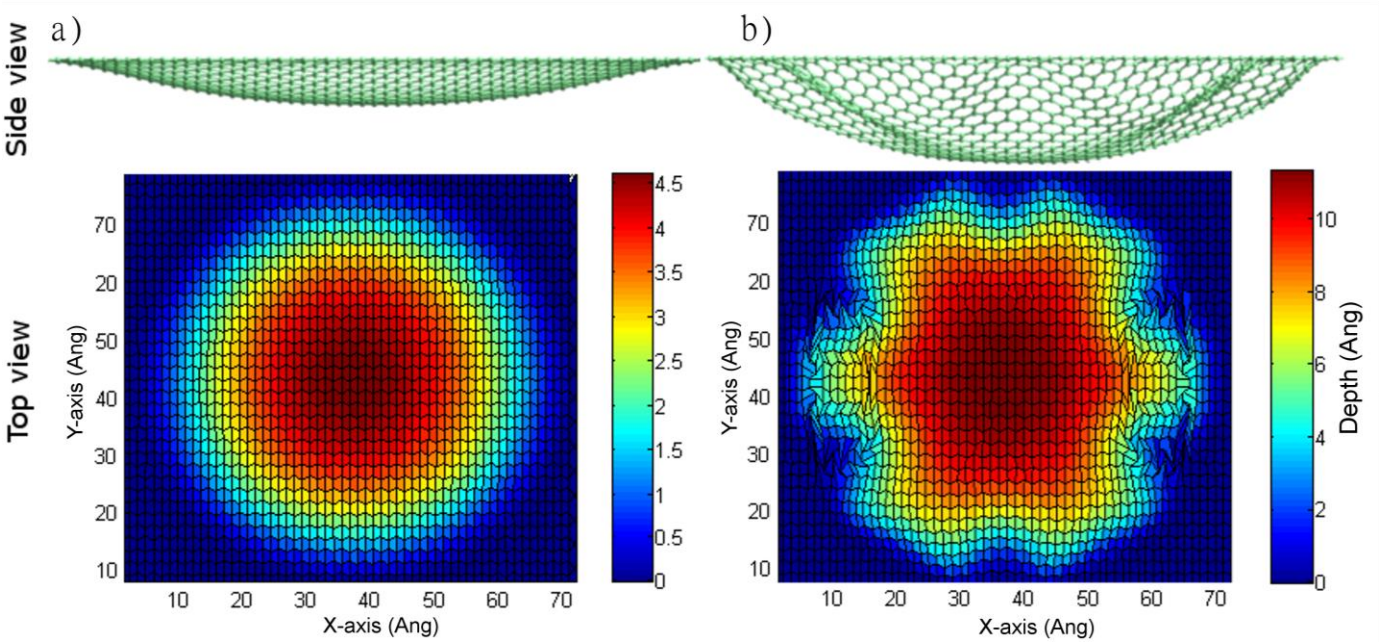

Figure 2. The spontaneous indentation of the unconstrained graphene in a 2160 atom sheet when subject to **(a)** 3% and **(b)** 7% biaxial compressive strain. The side view depicts the atomistic "nano bowl" structure. The top view depicts a colour plot of the indentation depth in angstrom.

Table 2. Values for Young's modulus, E, and sheet pretension, σ(fit), derived by fitting equation 1 to the load versus indentation curves similar to figure 3 (a), and the 'true' value from the stress tensor, σ(calculated). Results are given for empirical force field, $E_{Empirical}$, and DFT, E_{DFT}, calculations The first column gives the actual pre-tension applied to the membrane in each case, negative values correspond to tensile strain and positive values to compressive strain applied prior to indentation. The popping indentation for the compressed sheet's are also given in the last column.

	$E_{Empirical}$ (Nm^{-1})	E_{DFT} (Nm^{-1})	$\sigma_{Empirical}$ (fit) (Nm^{-1})	σ_{DFT} (fit) (Nm^{-1})	$\sigma_{Empirical}$ (calculated) (Nm^{-1})	σ_{DFT} (calculated) (Nm^{-1})

In-plane	306.0	330.0	-	-	-	-
Ten-7%	344.3±1.0	304.4±1.8	2.23±0.04	2.90±0.07	18.18	16.95
Ten-5%	338.8±1.9	274.2±1.8	0.66±0.10	2.56±0.09	14.69	12.36
Ten-3%	330.1±2.0	277.0±1.2	-0.51±1.10	0.87±0.06	9.99	7.27
Ten-1%	292.0±1.0	257.8±0.4	-1.78±0.04	-1.29±0.03	3.78	0.57
0%	282.8±0.4	253.5±0.1	-2.90±0.02	-2.76±0.01	0.00	-3.30
Com-1%	272.7±2.2	245.2±1.1	-3.79±0.13	-3.43±0.07	-4.30	-7.64
Com-3%	250.2±2.8	226.4±2.0	-5.39±0.16	-4.46±0.13	-14.70	-17.63
Com-5%	252.4±2.5	206.1±2.9	-8.63±0.19	-5.61±0.19	-28.00	-29.69
Com-7%	243.1±1.6	207.1±1.8	-11.86±0.17	-8.07±0.16	-44.88	-43.53
Literature	340[a]	-	0.34[a]	-	-	-

[a] Experimental [4]

Comparing first the Young's modulus determined directly from in-plane strain of the small, 4 atom unit cell, to values deduced by fitting the load indentation curve for zero pretension we see in table 2 that the latter values are considerably reduced both for the empirical and ab initio calculation. The DFT calculations are significantly worse in this regard. However it must be remembered that the DFT calculation of the membrane is not fully relaxed as can be seen from the calculated stress values where there is still a residual tensile compressive stress of $3.30 N m^{-1}$ corresponding to a value of 0.82% tensile strain, at supposedly zero pretension. However even for the case where the stress is near zero ($0.57 N m^{-1}$) the deduced value of Young's modulus is still substantially lower than that from the direct, in-plane strain calculation on the small unit cell. It is important to realize that identical methods are being compared here, and that these results are a test of the continuum clamped membrane model. If this model is valid then one might expect values of Young's modulus derived by fitting equation (1) to the load versus indentation curve and the value derived directly by in-plane strain applied to a small unit cell would be the same, at least within the numerical accuracy of the methods and the fitting procedure. Numerical accuracy is high in these calculations as we have used a set of computational conditions that are well converged, the fitting errors determined using the jackknife methodology[43] show that the elastic constants can be derived from these calculations to considerable precision. The difference between the two approaches observed here could be indicative of an underestimation by the indentation method similar to those proposed by *Tan et al* [18]. This is supported further by the variation in Young's modulus derived from load versus indentation curves calculated for different pretension values as shown in figure 3 (b). The variation in Young's modulus could be explained by the inability of the pretension term in the indentation model to accurately capture the strain present in the sheet as seen in figure 3 (c). While Tan *et al*[18] propose an alternate spherical load model for simulated indentations which requires a correction factor to the Young's modulus, $(R/A)^{\frac{1}{4}}$ where R is the indenter radius and A well radius, this gives E = 486 Nm^{-1} and 383 Nm^{-1} for our empirical and *ab initio* calculations respectively.

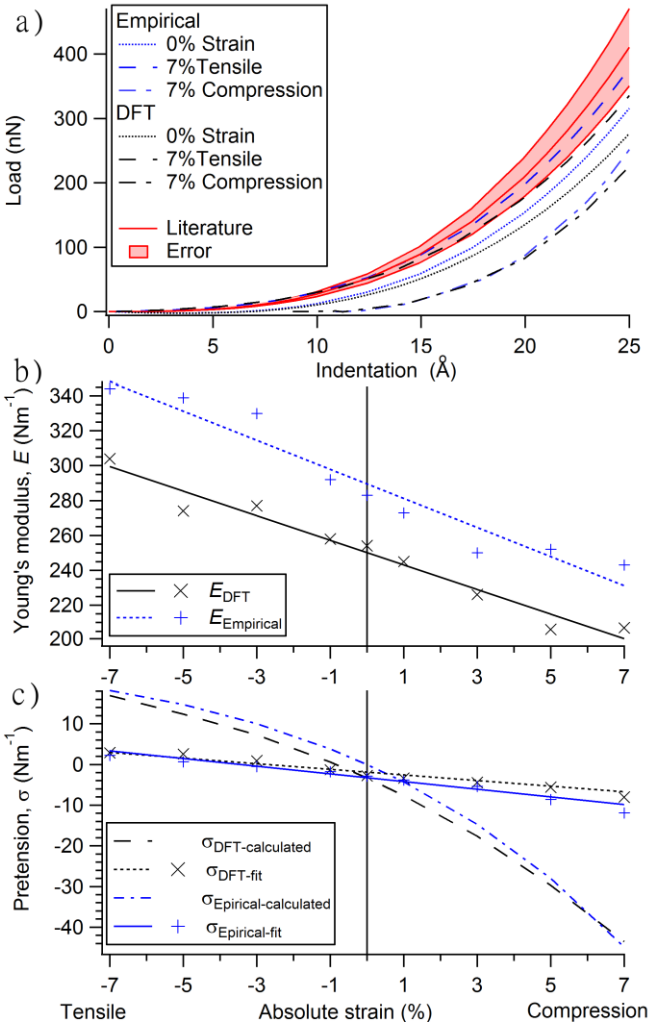

Figure 3. (a) The load Vs indentation curves from empirical simulations and AFM experiment[4] **(b)** The Young's modulus determined from fitting equation (1) to load Vs indentation data using empirical force field (+) and density functional theory (×) methodology as a function of absolute strain uniaxial strain on the graphene. **(c)** The pretention determined by fitting equation (1) to the load vs indentation data for empirical (+) and DFT (×) as well as the pretention calculated directly from the x and y stress tensor components for empirical and DFT.

In the experiments of *Lee et al* the load indentation curve is measured using an AFM, the Young's Modulus and pretension are determined by fitting equation 1 to this curve. The pre-tension in their membranes was found to be in the range of 0.07 – 0.74 Nm^{-1}. It was concluded that the free-standing graphene was initially in a compressed state to compensate for the observation of the graphene membrane adhering down the sides of the well for up to 10nm, pulling the sheet tort, and giving rise to a final tensile strain in the suspended membrane of ~2%. From our results we could provide an alternate interpretation. The pretension determined by fitting actually corresponds to a tensile strain of ~4%, meaning the graphene may have initially been relaxed or even under a slight tensile strain.

Their results show a reasonable variation in the Young's modulus with an average value of 340 +/- 50 Nm^{-1} in good agreement with both our own and literature calculations from a small unit cell. Our results would suggest that this agreement is fortuitous. The indentation model is inadequate and tends to underestimate the Young's modulus furthermore the correlation of the experimental value with small unit cell calculations could due to a compensating tensile strain which has the effect of increasing value of Young's modulus determined by equation (1). If we assume the graphene does truly have a ~4% tensile strain to match our interpretation of *lee et al*s fitted pretension then we would also expect a Young's modulus of 330-338 Nm^{-1} in good agreement with the experimental values.

4. Conclusion

Simulations using empirical and, for the first time, *ab initio* methods were performed to investigate the elastic properties and morphology of indented graphene membranes. It was observed that the presence of compressive strain in the sheet prior to indentation can lead to spontaneous indentation of the sheet which, in the case of strain greater than 3%, leads to the formation of wrinkles. Furthermore this morphology seems to have relatively little effect on calculated Young's modulus.

Values of Young's modulus determined directly by straining a small unit cell in-plane and by fitting a classical, continuum model to load versus indentation curves are quite different. The derived value of Young's modulus from this indented elastic membrane model shows a variation of approximately 30% for different pre-tensions in the membrane, despite the fact that the classical model contains a term that explicitly accounts for this pretension. Values of the pretension derived from the fitted model and from direct calculation are also in disagreement. It would seem, from these, results that the classical membrane model of *Wan et al* is therefore not adequate to describe indentation of a real graphene membrane with nanometre dimensions. This may be due to neglecting of bending rigidity, or the assumption of isotropic stress in the membrane that is independent of radial distance from the film centre. This difference could not be reconciled with the recently proposed spherical load model[18] however could be resolved by the presence of tensile strain in the graphene sheet. Instead we propose an underestimation of the indentation model that was compensated for by the presence of tensile strain. Additionally, a comparison with *ab initio* results suggests the inability of the Brenner potential to fully describe out-of plane bending at larger indentations.

Acknowledgements

This research was undertaken with the assistance of resources provided at the NCI National Facility systems at the Australian National University through the National Computational Merit Allocation Scheme supported by the Australian Government.

References

[1] Novoselov K S, Geim A K, Morozov S V, Jiang D, Zhang Y, Dubonos S V, Grigorieva I V and Firsov A A 2004 Electric field effect in atomically thin carbon films. *Science* **306** 666–9

[2] Berger C, Song Z, Li T, Li X, Ogbazghi A Y, Feng R, Dai Z, Marchenkov A N, Conrad E H, First P N and Heer W A De 2004 Ultrathin Epitaxial Graphite : 2D Electron Gas Properties and a Route toward Graphene-based Nanoelectronics *J. Phys. Chem. B* **108** 19912–6

[3] Casiraghi C, Hartschuh A, Lidorikis E, Qian H, Harutyunyan H, Gokus T, Novoselov K S and Ferrari A C 2007 Rayleigh imaging of graphene and graphene layers. *Nano letters* **7** 2711–7

[4] Lee C, Wei X, Kysar J W and Hone J 2008 Measurement of the elastic properties and intrinsic strength of monolayer graphene. *Science* **321** 385–8

[5] Geim A K and Novoselov K S 2007 The rise of graphene. *Nature materials* **6** 183–91

[6] Wang X, Zhi L and Müllen K 2008 Transparent, conductive graphene electrodes for dye-sensitized solar cells. *Nano letters* **8** 323–7

[7] Fair K, Cui X, Li L, Shieh C, Zheng R, Liu Z, Delley B, Ford M, Ringer S and Stampfl C 2013 Hydrogen adsorption capacity of adatoms on double carbon vacancies of graphene: A trend study from first principles *Phys Rev B* **87** 014102

[8] Liu G, Ahsan S and Khitun A 2013 Graphene-Based Non-Boolean Logic Circuits *arXiv:1308.2931 (unpublished)* 1–25

[9] Hancock Y 2011 The 2010 Nobel Prize in physics — ground-breaking experiments on graphene *J. Phys. D: Appl. Phys.* **44** 473001

[10] Lee J-U, Yoon D and Cheong H 2012 Estimation of Young's modulus of graphene by Raman spectroscopy. *Nano letters* **12** 4444–8

[11] Hossain M Z 2010 Quantum conductance modulation in graphene by strain engineering *App. Phys. Lett.* **96** 143118

[12] Griffith A A 1921 The Phenomena of Rupture and Flow in Solids *Phil. Trans. R. S. A.* **221** 163–98

[13] Al-Jishi R and Dresselhaus G 1982 Lattice-dynamical model for graphite *Phys. Rev. B.* **26** 4514

[14] Komaragiri U, Begley M R and Simmonds J G 2005 The Mechanical Response of Freestanding Circular Elastic Films Under Point and Pressure Loads *J. App. Mech.* **72** 203

[15] Wan K-T, Guo S and Dillard D a. 2003 A theoretical and numerical study of a thin clamped circular film under an external load in the presence of a tensile residual stress *Thin Solid Films* **425** 150–62

[16] Yakobson B, Brabec C and Bernholc J 1996 Nanomechanics of carbon tubes: Instabilities beyond linear response. *Phys. Rev. Lett.* **76** 2511–4

[17] D. H. Robertson, D. W. Brenner W M 1992 Energetics of nanoscale graphitic tubules *Phys. Rev. B.* **45** 592–5

[18] Tan X, Wu J, Zhang K, Peng X, Sun L and Zhong J 2013 Nanoindentation models and Young's modulus of monolayer graphene: A molecular dynamics study *App. Phys. Lett.* **102** 071908

[19] Neek-Amal M and Peeters F M 2010 Nanoindentation of a circular sheet of bilayer graphene *Phys. Rev. B.* **81** 1–6

[20] Neek-amal M and Asgari R 2011 Nano-indentation of circular graphene flakes *arXiv:0903.5035 (unpublished)* 1–4

[21] Wang Q 2010 Simulations of the bending rigidity of graphene *Phys. Lett. A.* **374** 1180–3

[22] Lu Q, Arroyo M and Huang R 2009 Elastic bending modulus of monolayer graphene *J. Phys. D* **42** 102002

[23] Huang X and Zhang S 2011 Morphologies of monolayer graphene under indentation *Mod. Sim. Mat. Sci. Eng.* **19** 054004

[24] Zhang Z, Duan W H and Wang C M 2012 Tunable wrinkling pattern in annular graphene under circular shearing at inner edge. *Nanoscale* **4** 5077–81

[25] Wang C, Lan L and Tan H 2013 The physics of wrinkling in graphene membranes under local tension. *Phys. Chem. Chem. Phys.* **15** 2764–73

[26] Wang C, Mylvaganam K and Zhang L 2009 Wrinkling of monolayer graphene: A study by molecular dynamics and continuum plate theory *Phys. Rev. B.* **80** 1–5

[27] Duan W H and Wang C M 2009 Nonlinear bending and stretching of a circular graphene sheet under a central point load. *Nanotechnology* **20** 075702

[28] Xu X and Liao K 2001 Molecular and continuum mechanics modeling of graphene deformation *Mater. Phys. Mech.* **4** 148–51

[29] Wei X and Kysar J W 2012 Experimental validation of multiscale modeling of indentation of suspended circular graphene membranes *Int. J. Solids Struct.* **49** 3201–9

[30] Wang R, Wang S, Wu X and Liang X 2010 First-principles calculations on third-order elastic constants and internal relaxation for monolayer graphene *Physica B* **405** 3501–6

[31] Cadelano E, Palla P, Giordano S and Colombo L 2009 Nonlinear Elasticity of Monolayer Graphene *Phys. Rev. Lett.* **102** 1–4

[32] Xu M, Paci J T, Oswald J and Belytschko T 2012 A constitutive equation for graphene based on density functional theory *Int. J. Solids Struct.* **49** 2582–9

[33] Soler M, Artacho E, Gale J D, Garc A, Junquera J, Ordej P and Daniel S 2002 The SIESTA method for ab initio order- N materials *J. Phys.: Condens. Matter* **2745**

[34] Izquierdo J, Vega A and Balbás L 2000 Systematic ab initio study of the electronic and magnetic properties of different pure and mixed iron systems *Phys. Rev. B.* **61**

[35] Perdew J, Burke K and Ernzerhof M 1996 Generalized Gradient Approximation Made Simple. *Phys. Rev. Lett.* **77** 3865–8

[36] Gale J 1997 GULP: A computer program for the symmetry-adapted simulation of solids *J. Chem. Soc., Faraday Trans.* **93** 629–37

[37] Gale J D 2005 GULP: Capabilities and prospects *Z. Krist.* **220** 552–4

[38] Gale J D and Rohl A L 2003 The General Utility Lattice Program (GULP) *Molelcular Simulations* **29** 291–341

[39] Brenner D 1990 Empirical potential for hydrocarbons for use in simulating the chemical vapor deposition of diamond films *Phys. Rev. B* **42**

[40] Abedpour N, Neek-Amal M, Asgari R, Shahbazi F, Nafari N and Tabar M 2007 Roughness of undoped graphene and its short-range induced gauge field *Phys. Rev. B.* **76** 195407

[41] Wei X, Fragneaud B, Marianetti C and Kysar J 2009 Nonlinear elastic behavior of graphene: Ab initio calculations to continuum description *Phys. Rev. B* **80** 205407

[42] Neek-Amal M and Peeters F M 2011 Buckled circular monolayer graphene: a graphene nano-bowl. *J. Phys.: Condens. Matter* **23** 045002

[43] Gammon S D and Ha C 1998 Non linear Least-Squares Curve Fitting with Microsoft Excel Solver *J. Chem. Ed.* **75** 119–21